Potential energy curves of the ground, excited, and ionized states of Ar_2 studied by the symmetry adapted cluster-configuration interaction theory

Yoshihiro Mizukami and Hiroshi Nakatsuji[a)]
Division of Molecular Engineering, Graduate School of Engineering, Kyoto University, Kyoto 606, Japan

(Received 29 August 1989; accepted 9 February 1990)

Symmetry adapted cluster-configuration interaction theory is applied to the calculation of potential energy curves for the ground, excited, and ionized states of Ar_2. The excited states studied here dissociate into $Ar(3p^6)$ + $Ar(3p^5 4s^1)$ and $Ar(3p^6)$ + $Ar(3p^5 4p^1)$. Spin–orbit coupling is included by a semiempirical method. The present results, especially for the 4*s* Rydberg states, compare very well with the experimental results of absorption and emission spectra. Some new assignments of the observed spectra are given, particularly for excitations from bound excited states of Ar_2.

I. INTRODUCTION

In their pioneering work on the vacuum ultraviolet (VUV) spectra in 1970, Tanaka and Yoshino[1] assigned nine absorption band systems for the Ar dimer. Their vibrational analysis gave a very accurate estimate of the ground-state potential curve. They also showed, for the first time, accurate information for some excited states. The development of VUV laser spectroscopy thereafter has made it possible to obtain very high-resolution spectra of rare-gas dimers.[2]

Recently, Herman, Madej, LaRocque, and Stoicheff[3,4] have reported rovibronic structures of Ar_2 in the laser-induced fluorescence spectra for the excitations, $A(1_u)$, $B(0_u^+)$, $C(0_u^+) \leftarrow X(0_g^+)$, using an isotopic species $^{36}Ar^{40}Ar$. Their rovibrational analysis showed that the $A(1_u)$ state in high vibrational levels follows Hund's case (c), where the atomic spin-orbit (SO) coupling is strong. They suggested reliable potential energy curves of the $X(0_g^+)$ and $C(0_u^+)$ states near the potential minimum of the ground state. However, information of the potential well of both the $A(1_u)$ and $B(0_u^+)$ states remains unknown experimentally.

On the other hand, theoretical studies on the excited sates of rare- gas dimers have been developed ever since the frontier work of Mulliken on Xe_2.[5] For Ar_2, the first *ab initio* configuration interaction (CI) calculations of the excited states were reported by Saxon and Liu in 1974.[6] They obtained the potential curves of the $^3\Sigma_u^+$ and $^3\Sigma_g^+$ states using a Slater-type orbital (STO) basis set. Spiegelmann and Malrieu studied the potential curves of the excited states using pseudopotential and Gaussian-type orbital (GTO) basis sets by an approximate CI method.[7] Later they included spin–orbit coupling by the semiempirical method of Cohen and Schneider for the 4*s* Rydberg states.[8] Spiegelmann and Gadea also reported many potential curves of 4*s* and 4*p* Rydberg states.[9] Yates *et al.* used a STO basis set with a refined effective core potential and calculated the potential curves of the 4*s* and 4*p* Rydberg states by the polarization CI method.[10] These theoretical studies were able to give global features of the potential energy curves.

Rare-gas dimers are weakly interacting systems and it is not easy to obtain quantitatively reliable potential curves. For the excited states of Ne_2, Grein, Peyerimhoff, and Buenker reported multireference double excitation (MRD)—CI calculations with extended basis sets.[11,12] Even such high-level calculations have shown inconsistencies with the experimental spectra. For Ar_2, reliable potential curves, which are consistent with radiative experiments especially with those very recently reported by Herman *et al.*,[3,4] remain to be calculated.

Here, we perform all-electron *ab initio* calculations of the ground, excited, and ionized states of Ar_2 using a large GTO basis set by symmetry adapted cluster (SAC) expansion[13] and SAC-CI[14] methods. Our results should be very accurate, especially for the 4*s* Rydberg states, since they give spectroscopic properties that agree very well with the available experimental results.

II. CALCULATIONAL METHOD

To calculate reliable potential curves of the ground and excited states of van der Waals molecules, it is not only necessary to include a sufficient number of electron correlations, but also to calculate electron correlations of the ground and excited states with balanced accuracy. For this purpose, the SAC and SAC-CI theories[13,14] are very suitable.[15,16] We only note here that, for van der Waals molecules, the Hartree–Fock (HF) configuration is dominant in the ground-state wave function throughout the interaction, so that the SAC wave function is well defined at all internuclear distances. In the present calculations, we have used the program system, SAC85.[17]

The interaction in the van der Waals molecule is very weak and the description of the interactions in the excited states requires relatively diffuse basis set, which are less important for the description of the ground state. The use

[a)]Present address: Department of Synthetic Chemistry, Faculty of Engineering, Kyoto University, Kyoto 606, Japan.

 0021-9606/90/106084-09$03.00

TABLE I. Calculated total energies of the ground state $X(^1\Sigma_g^+)$ of Ar_2 at various internuclear separations.

R (bohr)	Energy (au)[a]
4.0	−0.695 06
4.5	−0.771 36
4.6	−0.781 33
4.65	−0.785 32
4.7	−0.788 85
4.77	−0.793 26
5.0	−0.805 59
5.5	−0.819 38
6.0	−0.825 55
7.0	−0.829 44
8.0	−0.830 86
9.0	−0.829 67
12.0	−0.830 28

[a]The reference energy is −1053 hartree.

of a good basis set is the first step for obtaining reliable results. Here, the core and valence parts of Ar_2 are represented by the contracted Gaussian basis set (12*s*9*p*/6*s*5*p*) of McLean and Chandler.[18] Three sets of *d* functions are added as polarization functions. Two ($\zeta_d = 0.950$, 0.263) are taken from Huzinaga's table[19] and one ($\zeta_d = 0.169\ 87$) is added for describing weak interactions.[8] Two *s* ($\zeta_s = 0.040\ 201, 0.017\ 125$) and two *p* ($\zeta_p = 0.040\ 201, 0.017\ 125$) functions due to Castex *et al.*[8] are used for representing the Rydberg 4*s* and 4*p* orbitals. Further, two *s* functions ($\zeta_s = 0.032\ 538, 0.012\ 844$) are added to reinforce the Rydberg *s* orbitals. They are determined by the method of Dunning and Hay.[20]

The all-electron HF wave function for the ground state of Ar_2 is calculated by the program GAMESS.[21] It consists of 18 occupied orbitals and 80 unoccupied orbitals. For the SAC and SAC-CI calculations, we use the highest eight occupied orbitals ($3s\sigma_g^2$, $3s\sigma_u^2$, $3p_z\sigma_g^2$, $3p_x\pi_u^2$, $3p_y\pi_u^2$, $3p_x\pi_g^2$, $3p_y\pi_g^2$, $3p_z\sigma_u^2$) and the lowest 50 unoccupied orbitals as active orbitals. In the SAC method, one and two electron excitation operators are treated as linked operators and products of two electron excitation operators as unlinked operators. The configuration selection is performed for the linked excitation operators with $\lambda_g = 3 \times 10^{-5}$ hartree and $\lambda_e = 5 \times 10^{-5}$ hartree.[15] In the unlinked terms, we have included only such operators whose single and double excitation (SD)CI coefficients for the ground state are larger than 5×10^{-3} in SAC and 1×10^{-3} in SAC-CI.

III. POTENTIAL CURVES WITHOUT SPIN–ORBIT COUPLING

The potential curve of the ground state as calculated by the HF method has no minimum, since this method is unable to describe van der Waals interactions. On the other hand, the ground-state curve calculated by the SAC method has a shallow van der Walls minimum at $R_{min} = 8.1$ bohr, compared with the experimental value of 7.107 bohr.[4] The depth of the potential well is calculated to be 15.9 meV in comparison with the experimental value,[4] 12.3 meV. Total energies of the ground state calculated by the SAC method at various distances are listed in Table I.

We have calculated 24 singlet and triplet excited states

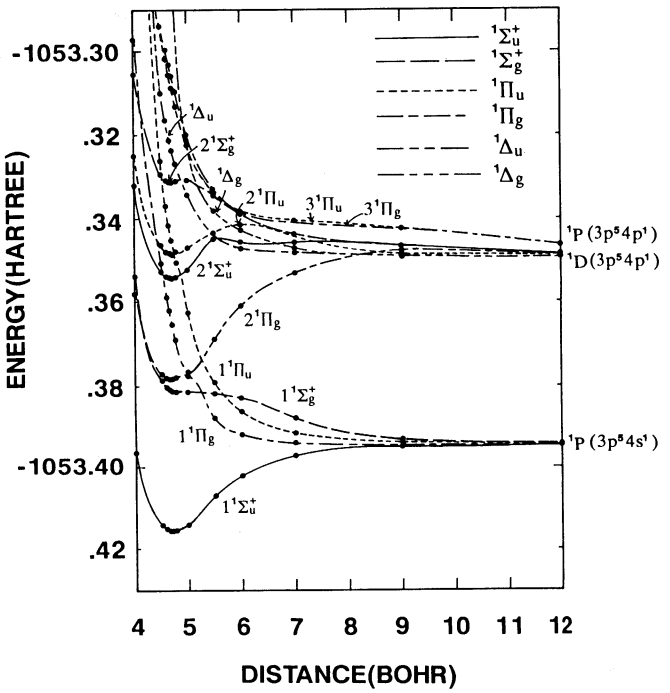

FIG. 1. Potential energy curves of the singlet excited states of Ar_2 calculated without including SO interactions.

by the SAC-CI method. Figures 1 and 2 show the potential curves of the singlet and triplet excited states, respectively. The lowest four curves dissociate into the state, $Ar(3p^6) + Ar(3p^54s^1)$ and the upper eight curves into $Ar(3p^6) + Ar(3p^54p^1)$. These states are the so-called long-range resonance interaction states.[22]

Many avoided crossings occur because these potential curves are adiabatic. A useful survey of the diabatic potential curves of Ne_2 is given by Grein *et al.*[11] Their discussion

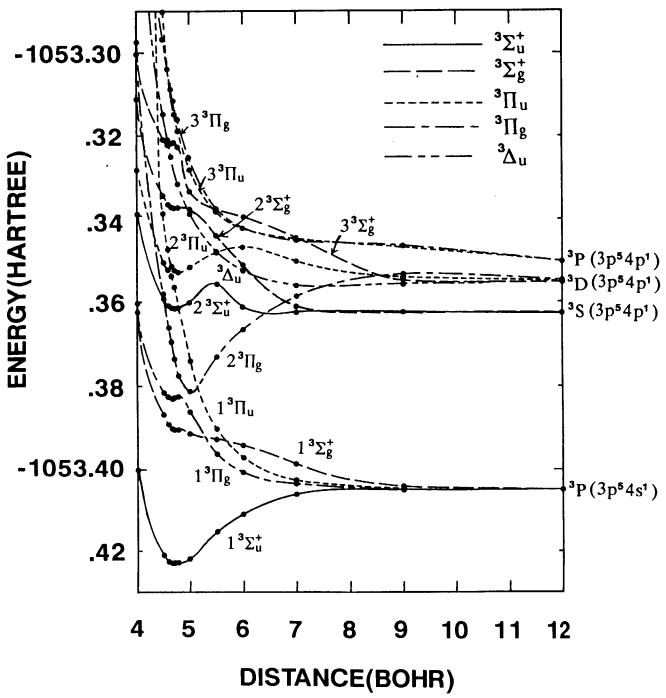

FIG. 2. Potential energy curves of the triplet excited states of Ar_2 calculated without including SO interactions.

TABLE II. Characteristic distances in the potential curves of the various excited states of Ar_2 calculated without including SO interactions.

State	R_{min} (bohr) singlet	R_{min} (bohr) triplet	Main configuration $R < R_{hump}$ or R_{shoul}	Main configuration $R > R_{hump}$ or R_{shoul}	R_{hump} or R_{shoul} (bohr) singlet	R_{hump} or R_{shoul} (bohr) triplet
$1\Sigma_g^+$	4.70	4.71	$\sigma_u \rightarrow 4p\sigma_u$	$\sigma_g \rightarrow 4s\sigma_g$	4.79(h)[c]	4.77(h)[c]
$2\Sigma_g^+$	4.68	4.71	$\sigma_u \rightarrow 5p\sigma_u$	$\pi_u \rightarrow 4p\pi_u$	4.95(h)	4.82(h)
$3\Sigma_g^+$[a]		4.60	$\sigma_u \rightarrow 6p\sigma_u$	$\sigma_g \rightarrow 4p\sigma_g$		4.70(h)
$1\Sigma_u^+$	4.65	4.66	$\sigma_u \rightarrow 4s\sigma_g$			
$2\Sigma_u^+$	4.66	4.66	$\sigma_u \rightarrow 5s\sigma_g$	$\pi_g \rightarrow 4p\pi_u$	5.65(h)	5.50(h)
$1\Pi_g$	4.66	4.68	$\sigma_u \rightarrow 4p\pi_u$	$\pi_g \rightarrow 4s\sigma_g$	4.93(h)	4.77(h)
$2\Pi_g$	5.10	5.00	$\pi_g \rightarrow 4s\sigma_g$			
			$\sigma_u \rightarrow 4p\pi_u$			
$3\Pi_g$			$\pi_g \rightarrow 4p\sigma_g$			
$1\Pi_u$	4.66		$\sigma_u \rightarrow 4d\pi_g$	$\pi_u \rightarrow 4s\sigma_g$	4.68(h)	4.60(s)
$2\Pi_u$	4.84	4.79	$\pi_u \rightarrow 4s\sigma_g$	$\sigma_g \rightarrow 4p\pi_u$		
			$\pi_u \rightarrow 4s\sigma_g$			
$3\Pi_u$			$\pi_g \rightarrow 4p\sigma_u$			
			$\pi_u \rightarrow 4p\sigma_g$			
Δ_u			$\pi_g \rightarrow 4p\pi_u$			
Δ_g[b]			$\pi_g \rightarrow 4p\pi_g$		5.95(s)	

[a]Calculated for only the triplet state.
[b]Calculated for only the singlet state.
[c]h and s in parentheses mean hump and shoulder, respectively.

is also applicable to Ar_2. For rare-gas excimers, Mulliken[5] proposed an excellent interpretation for the shapes of the potential energy curves. This is as follows: A rare-gas excimer has an electron in a Rydberg orbital which feels a potential of the ionic core X_2^+ (X = Ne, Ar, Kr, and Xe). The ground state of a rare-gas dimer has four higher occupied molecular orbitals (MOs), $p\sigma_u$, $p\pi_g$, $p\pi_u$, and $p\sigma_g$, from which an electron is excited into the Rydberg orbital. As the binding energy of the Rydberg orbital is small, the ionic core is responsible for the bonding of the system. An excitation from the antibonding MO(σ_u, π_g) makes the system stable and that from the bonding MO(π_u, σ_g) makes it unstable. Thus, the potential curves for the excitations from the σ_u and π_g MOs will be bound and those from the π_u and σ_g MOs should be essentially repulsive. The depth of the potential minimum should be larger for the excited states from the σ_u MO than from the π_g MO, because the antibonding nature is larger in the σ_u MO than in the π_g MO.

Main configurations and the characteristic distances of the potential curves are summarized in Table II. R_{min}, R_{hump}, and R_{should} denote the nuclear distances at the minimum, hump, and shoulder, respectively, in a curve. Main configurations of the excited states often change near the avoided crossings, namely at the humps or shoulders. This change is also shown in Table II.

As shown in Figs. 1 and 2, the lowest $1\Sigma_u^+$ state is a bound state and has a potential minimum at 4.65 bohr for the singlet state and at 4.66 bohr for the triplet state. The dominant excitation configuration is $3p\sigma_u \rightarrow 4s\sigma_g$ over all of the potential curve. No avoided crossing occurs for these states. The potential curves of the singlet and triplet $2\Sigma_u^+$ states, which are mainly $3p\sigma_u \rightarrow 5s\sigma_g$ at shorter distances, have their first minima at 4.66 bohr (both singlet and triplet, about the same distances as those of the $1\Sigma_u^+$ states) and then show humps due to the avoided crossing and the nature of the main excitation configurations changes drastically. After the hump, the repulsive excitation configuration, $3p\pi_g \rightarrow 4p\pi_u$, becomes dominant. All of the Σ_g^+ curves obtained here are repulsive except for the positions of small humps, shoulders, and shallow wells at short distances of about 4.7 bohr.

The $1\Pi_g$ and $2\Pi_g$ states show a typical avoided crossing at about 5.0 bohr. This is due to the mixing of the $3p\sigma_u \rightarrow 4p\pi_u$ and $3p\pi_g \rightarrow 4s\sigma_g$ configurations. After the avoided crossing, the $1\Pi_g$ state dissociates repulsively into the $Ar(3p^6) + Ar(3p^5 4s^1)$ resonance state, and the $2\Pi_g$ state rises sharply, leaving the potential minimum at the avoided-crossing distance, and dissociates into the $Ar(3p^6) + Ar(3p^5 4p^1)$ state. The $3\Pi_g$ state is repulsive all over the curve. The $1\Pi_u$ and $2\Pi_u$ states also show an avoided crossing; The $1\Pi_u$ state shows a repulsive dissociation and the $2\Pi_u$ state has a shallow minimum at about 4.8 bohr. The $3\Pi_u$ state is repulsive throughout the curve. The Δ_u and Δ_g states are also repulsive throughout. Spiegelmann *et al.*[9] reported a potential minimum at short distance for the Δ_u state, but we do not obtain it.

Mulliken[22] studied the asymptotic behavior of the potential curves of homopolar diatomic molecules that dissociate into resonance states, i.e., one in the ground state and the other in the excited state at large separations. His rule shows that the Σ_u^+, Π_g, and Δ_u states should be attractive and the Σ_g^+, Π_u, and Δ_g states be repulsive at large separations. Our results almost agree with his rule with a few exceptions. One disagreement is seen for the third Π_g state, which is expected to be attractive but was calculated to be repulsive in our curves. This is because the $2\Pi_g$ and $3\Pi_g$ states (both singlet and triplet) suffer an avoided crossing at large separations; namely the $3\Pi_g$ state should have a shallow minimum at large separations. Yates *et al.*[10] also obtained a repulsive dissociation curve for the $3\Pi_g$ state.

IV. POTENTIAL CURVES WITH SPIN–ORBIT COUPLING

Cohen and Schneider[23] (CS) proposed a useful, semiempirical method for estimating the SO interactions in rare-gas excimers. It is based on the atoms-in-molecule idea. At the separated atom limit, their method coincides with the treatment of the SO coupling for atoms.[24] For the excited states of Ne_2, Grein, Peyerimh- off, and Klotz[25] compared the CS method with their *ab initio* study using the SO Hamiltonian by the Breit–Pauli formulation and concluded that the CS method is a reliable approximation.

We calculate the SO coupling constant for the 4*s* Rydberg states as $\zeta 3_p = 4.282\,67 \times 10^{-3}$ hartree from the energy difference between the $3p^5 4s(^3P_2)$ and $3p^5 4s(^3P_0)$ states of the Ar atom using Moore's table:[26]

$$\zeta 3_p = (2/3)[E(^3P_2) - E(^3P_0)].$$

For the $Ar(3p^6) + Ar(3p^5 4s^1)$ system, we obtained 16 curves after including the SO coupling. The potential curves of the ungerade and gerade states are shown in Fig.

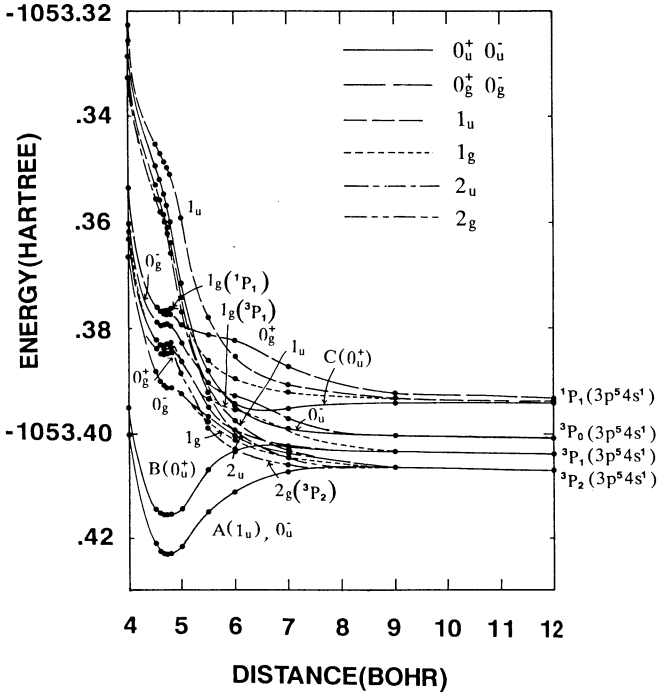

FIG. 3. Potential energy curves of the 4*s* Rydberg excited states of Ar_2 calculated with SO interactions.

3. These potential curves dissociate into the $Ar(^1S_0)$ + $Ar(^3P_{2,1,0})$ and $Ar(^1S_0)$ + $Ar(^1P_1)$ states, where the four different atomic limits of Ar_2 correspond to the molecular states as follows:

$$Ar(^1S_0) + Ar(^3P_2) \quad 0_u^-, 1_u, 2_u, 0_g^-, 1_g, 2_g,$$

$$Ar(^1S_0) + Ar(^3P_1) \quad 0_u^+, 1_u, 0_g^+, 1_g,$$

$$Ar(^1S_0) + Ar(^3P_0) \quad 0_u^-, 0_g^-,$$

$$Ar(^1S_0) + Ar(^1P_1) \quad 0_u^+, 1_u, 0_g^+, 1_g.$$

Hereafter, we use the notation like $1_g(^1P_1)$ in Fig. 3 for showing molecular 1_g state which dissociates into $Ar(^1S_0)$ and $Ar(^1S_0)$ and $Ar(^1P_1)$.

The energy levels[26] of the excited states of Ar atom are listed in Table III. Our results for Ar_2 at 12 bohr are also listed. They agree with the experimental values to within 420 cm^{-1}. This fact would be attributed to the size-consistency of the cluster expansion, although several approximations like configuration selection are introduced in the present calculations.

As shown in Fig. 3, there are four bound states in the present results; the first 0_u^-, $A(1_u)$, $B(0_u^+)$, and $C(0_u^+)$ states. The potential curves of the first 0_u^- and $A(1_u)$ states almost overlap each other at all nuclear separations. There is a metastable minimum in the $1_g(^1P_1)$ state. This originates from the avoided crossing between the $1\,^1\Pi_g$ and $2\,^1\Pi_g$ states.

TABLE III. The energy levels of the 4*s* Rydberg excited states of Ar_2 calculated at $R = 12$ bohr compared with the Ar atom spectra.

State	$Ar_2(R = 12$ bohr) calc(cm^{-1})	Ar atom expt(cm^{-1})[a]
$^3P_2$	92 904	93 143.80
$^3P_1$	93 564	93 750.64
$^3P_0$	94 284	94 553.71
$^1P_1$	95 820	95 399.87

[a]Reference 26.

The spectroscopic constants associated with each potential curve are calculated by the extended Morse fitting method of Hulburt and Hirschfelder.[27] The results for the adiabatic excitation energy T_e between lowest vibrational levels, the vibrational frequencies ω_e, $\omega_e\chi_e$, and the dissociation energy D_e are summarized in Table IV together with the experimental and previous theoretical results. The T_e value of the $C(0_u^+)$ state agrees well with the experimental value of Herman *et al.*[4] For the $A(1_u)$ and $B(0_u^+)$ states, the agreement is less satisfactory, probably because the experimental estimate is indirect and less reliable than that for the $C(0_u^+)$ state.[4] Recently, Shannon and Eden[28] observed intracavity laser absorption spectra from the $A(1_u)$ state to the Π_g state of the 5*p* Rydberg state. From vibrational analysis, they estimated the values of ω_e and $\omega_e\chi_e$ of the $A(1_u)$ state to be 297.2 and 3.3 cm^{-1}, respectively, and our results are 273.5 and 4.10 cm^{-1}, respectively. For the $C(0_u^+)$ state, Herman *et al.*[4] reported $\omega_e = 68.16$ and $\omega_e\chi_e = 4.631$ cm^{-1} and our results are $\omega_e = 69.8$ and $\omega_e\chi_e = 6.05$ cm^{-1}. The dissociation energy for the $A(1_u)$ state is calculated to be 3504 cm^{-1}, which is rather small in comparison with the experimental values, 6130[29] and 5643 cm^{-1}.[30] The theoretical result of Yates *et al.*[10] is 4194 cm^{-1}, which is also smaller than the experimental values. We note here that Tanaka *et al.*[1] pointed out a deviation of the $A(1_u)$ curve from the Morse curve. Care is needed to estimate the dissociation energy from the experimental extrapolation to the Morse curve for such a weakly interacting system.

V. ABSORPTION AND EMISSION SPECTRA INVOLVING GROUND STATE

In 1970, Tanaka and Yoshino[1] observed nine discrete band systems of the Ar dimer by the VUV spectroscopy. Recently, Herman, LaRocque, and Stoicheff[4] (HLS) investigated the detailed structures of the lowest three bands, $A(1_u)$, $B(0_u^+)$, and $C(0_u^+)$ by high-resolution VUV laser spectroscopy. For the $A(1_u)$ state, they assigned eight vibrational levels ($v' = 23$–30) from their vertical excitation spectra.

On the theoretical side, we have calculated the vibrational levels by numerically solving the Schrödinger equations for our potential curves of the $A(1_u)$, $B(0_u^+)$, and $C(0_u^+)$ states. The numerical method we have employed is the finite element method (FEM) of Sato and Iwata.[31] We first perform analytical fitting of the present curves to the extend-Morse functions, and taking a large number of representative points from the curves [e.g., for the $A(1_u)$ state, 25 points from 4.0–9.0 bohr with a spacing of 0.2 bohr], we perform the FEM analysis using the program DIAVIB coded by Sato.[32] For the $A(1_u)$ state we obtain 23 vibrational levels ($v' = 0$–22). The uppermost level is $v' = 22$ and this is different from the experimental one $v' = 30$. So we take our highest eight levels to compare with

TABLE IV. Spectroscopic constants of the 4s Rydberg excited states of Ar_2 with SO interactions. Experimental results are shown in parentheses.

State	T_e (cm^{-1})	R_{min} (bohr)	R_{hump} or R_{shoul} (bohr)	ω_e (cm^{-1})	$\omega_e\chi_e$ (cm^{-1})	D_e (cm^{-1})
$A(1_u)(^3P_2)$	89 625	4.66[b],4.69[c]		273.5	4.10	3504[b],4194[c]
	(~87 458)[a]			(297.2)[d]	(3.3)[d]	(6130)[e],(5643)[f]
$B(0_u^+)(^3P_1)$	91 307	4.65[b],4.67[c]	6.63(h)[g]	231.3	3.03	2499[b],3629[c]
	(~88 210)[a]					
$C(0_u^+)(^1P_1)$	95 557	6.50	4.60(s)[g]	69.8	6.05	423
	(95 033.6)[a]	(6.80)[a]		(68.16)[a]	(4.631)[a]	(465.8)[a]
$0_u^-(^3P_2)$	89 625	4.66				
$0_u^-(^3P_0)$			4.77(s)			
$1_u(^3P_1)$			4.77(s)			
$1_u(^1P_1)$			4.77(s)			
$2_u(^3P_2)$			4.77(s)			
$0_g^-(^3P_2)$	96 469	4.71	4.77(h)			
$0_g^-(^3P_0)$	98 998	4.68	4.77(h)			
$0_g^+(^3P_1)$	98 097	4.69	4.77(h)			
$0_g^+(^1P_1)$	99 429	4.68	4.77(h)			
$1_g(^3P_2)$	96 492	4.71	4.77(h)			
$1_g(^3P_1)$	98 186	4.68	4.77(h)			
$1_g(^1P_1)$	99 634	4.67	4.91(h)			
$2_g(^3P_2)$	97 867	4.68	4.77(h)			

[a]Reference 4.
[b]This work.
[c]Reference 10.
[d]Reference 28.
[e]Reference 29.
[f]Reference 30.
[g]h and s in parentheses mean hump and shoulder, respectively.

the experimental levels. The results are shown in Table V. Theoretical and experimental values agree to within 340 cm^{-1}.

The difference in the number of the vibrational levels estimated from the experiment ($n = 31$)[4] and from our theoretical curve ($n = 23$) is attributed to the difference in the nature of the fitting functions used in the experiment and in our calculations. That is, HLS[4] used the Morse function and we use the extended-Morse function. Indeed, we found that the Morse function is insufficient for fitting our calculated points, though the extended Morse function fits them very well. This implies that the potential curve of the $A(1_u)$ state rises more rapidly from the minimum and then approaches more quickly to the dissociation limit[27] than expected by the experimentalists.

TABLE V. Vertical transition energies from the $X(0_g^+)$ state to the $A(1_u)$ state.

expt (cm^{-1})[a]			calc(cm^{-1})		
v'[b]	Transition energy	Level spacing	v'[b]	Transition[c] energy	Level spacing
23	92 386.66		15	92 384	
24	92 524.48	137.82	16	92 490	106
25	92 653.11	128.3	17	92 580	94
26	92 771.44	118.3	18	92 654	74
27	92 879.06	107.62	19	92 710	56
28	92 974.82	95.76	20	92 749	39
29	93 056.86	82.04	21	92 772	23
30	93 123.65	66.79	22	92 784	12

[a]Reference 4.
[b]Vibrational level of the upper $A(1_u)$ state.
[c]Relative to the ground state energy $-1053.896\,25$ hartree at R_{min} (exptl) = 7.107 bohr.

HLS[4] also observed the transition frequencies from the ground state to the highest eight vibrational levels ($v' = 20$–27) of the excited $B(0_u^+)$ state. We have applied the FEM for numerically obtaining the vibrational levels of the $B(0_u^+)$ state. The number of the vibrational levels calculated from our curve ($n = 16$) is also different from that of the experiment ($n = 28$).[4] This is attributed to the same reason described above for the $A(1_u)$ state. We take our highest eight levels to compare with the experiment in Table VI. The agreements are to within 220 cm^{-1}. The level spacings are also compared with the experimental values. Our potential curve shows a hump at 6.50 bohr with the height of about 93 920 cm^{-1} from the ground state. Beyond the level $v' = 27$, there have been some discussions whether a hump exists or not.[1,4,8] Here we note that HLS[4] reported an unidentified band system at 106 nm, which is located immediately on the blue side of the band system of the $B(0_u^+)$ state. They considered that the potential well of this system is shallow and the well depth is $D_e \sim 50$ cm^{-1}. The largest observed frequency of this band is 93 822 cm^{-1}, which is comparable with the frequency 93 920 cm^{-1} at the hump of our potential curve. It is possible to

TABLE VI. Vertical transition energies from the $X(0_g^+)$ state to the $B(0_u^+)$ state.

Exptl (cm^{-1})[a]			Calc(cm^{-1})		
v' [b]	Transition energy	Level spacing	v' [b]	Transition[c] energy	Level spacing
20	92 769.25		8	92 773	
21	92 935.93	166.68	9	92 976	203
22	93 093.54	157.61	10	93 173	197
23	93 241.17	147.63	11	93 360	187
24	93 377.62	136.45	12	93 535	175
25	93 501.55	123.93	13	93 693	158
26	93 610.76	109.21	14	93 829	136
27	93 701.31	90.55	15	93 918	89

[a]Reference 4.
[b]Vibrational level of the upper $B(0_u^+)$ state.
[c]Relative to the ground state energy at R_{min} (exptl) = 7.107 bohr.

suppose that this band system is due to the second potential minimum of the $B(0_u^+)$ state, which is located just on the right of the hump.

For the $C(0_u^+)$ state, HLS[4] observed the absorption frequencies from the ground state to the lower vibrational levels ($v' = 0$–4), so that they could estimate reliable spectroscopic values for this system. We have calculated this quantity from our potential curve by the FEM analysis and compared them in Table VII. The agreement with experiment is very good.

We have used Hund's case(c) formula for including the SO coupling. Herman *et al.*[4] suggested from the analysis of their rovibronic spectra that Hund's case(c) is valid for the vibrational levels $v' > 17$ in the $A(1_u)$ state. The reliability of our results may suggest that Hund's case(c) is valid for both of the $B(0_u^+)$ and $C(0_u^+)$ states at intermediate and large nuclear separations.

The emission occurs from the two lowest excited states, the $A(1_u)$ and $B(0_u^+)$ states of Ar_2, to the repulsive ground state.[33] Two emission paths have been observed.[34] One has a short lifetime and so assigned as the emission from the second lowest excited state, the $B(0_u^+)$ state, since this state has singlet character. This emission is the one that is responsible for the laser light of this system observed at 1232–1274 Å (81 170–78 490 cm^{-1}).[35] Another emission has a longer lifetime and is assigned as the emission from the lowest excited state, $A(1_u)$, which has triplet character. This peak is broad[33] because of a rapid dissociation of the repulsive ground state.

TABLE VII. Vertical transition energies from the $X(0_g^+)$ state to the vibrational levels ($v' = 0$–3) of the $C(0_u^+)$ state.

Exptl (cm^{-1})[a]			Calc(cm^{-1})		
v' [b]	Transition energy	Level spacing	Transition[c] energy	Level spacing	
0	95 051.21		95 360		
1	95 110.06	58.85	95 417	57	
2	95 160.97	50.91	95 461	44	
3	95 203.58	42.61	95 495	34	

[a]Reference 4.
[b]Vibrational level of the upper $C(0_u^+)$ state.
[c]Relative to the ground state energy at R_{min} (exptl) = 7.107 bohr.

The transition energies of the emissions from the zero point vibrational levels of the $A(1_u)$ and $B(0_u^+)$ states are respectively 1256 Å (79 620 cm^{-1}) and 1232 Å (81 170 cm^{-1}) in the present calculations. These are comparable with the experimental wavelengths at maximum intensity, 1260 Å (79 400 cm^{-1}) for the $A(1_u)$ state and 1250 Å (80 000 cm^{-1}) for the $B(0_u^+)$ state.

VI. ABSORPTION SPECTRA FROM THE EXCITED STATES

The infrared absorption spectra from the metastable excited states, $^3\Sigma_u^+$ and $^1\Sigma_u^+$, of the rare-gas excimers, Ne_2, Ar_2, Kr_2, and Xe_2, were first observed by Arai and Firestone.[36] Later, Arai, Oka, Kogoma, and Imamura[37] observed fine structure for these spectra. They found two absorption band systems: the first band system has three wavelength maxima at 9600 Å (1.292 eV), 9754 Å (1.271 eV), and 9883 Å (1.255 eV). These are assumed to be the transitions between Rydberg s and p states. The second band system has two fine peaks at 12 380 Å (1.001 eV) and 12 660 Å (0.9793 eV). They are considered to be the electronic transitions within Rydberg s states and the vibrational structures. Both the first and second bands are assumed to be the absorptions from the $A(1_u)$ state, because the lifetime is almost the same as that of the emission from the $A(1_u)$ state to the ground state. For Ne_2, Iwata[38] reported *ab initio* CI calculations of many excited states in very good agreement with the experimental spectra and supported the assignments by Arai *et al.*[37] His conclusion is that the first band system is due to the transition, $2\,^3\Pi_g \leftarrow 1\,^3\Sigma_u$ and the second one to $1\,^3\Pi_g \leftarrow 1\,^3\Sigma_u$. While he did not include the SO interaction, it would become larger for Ar_2 than for Ne_2. So, we try to assign these two bands for the Ar excimer based on the potential curves, which include the SO interactions.

The second absorption band has two peaks. This may be due to vibration or due to different electronic excitations. In our calculations, there are three electronic states in the Rydberg s excited states whose transition energies from the $A(1_u)$ state are close to those of the observed second band. They are $0_g^+(^3P_1)$, $1_g(^3P_1)$, and $2_g(^3P_2)$ states. The $0_g^+(^3P_1)$ state originates from the $1\,^1\Sigma_g^+$ state and the $1_g(^3P_1)$ and $2_g(^3P_2)$ states from the $1\,^3\Pi_g$ state. The $A(1_u)$ state has $^3\Sigma_u^+$ character, so that the transitions from $A(1_u)$ to both $1_g(^3P_1)$and $2_g(^3P_2)$ states are dipole-allowed as triplet–triplet excitations. We may assign the absorption peaks with the wavelengths 12 380 Å (1.001 eV) and 12 660 Å (0.9793 eV) as being due to the transitions $1_g(^3P_1) \leftarrow A(1_u)$ or $2_g(^3P_2) \leftarrow A(1_u)$ and the hot bands of them. Figure 4 illustrates the absorptions from the excited $A(1_u)$ state. It can be seen that both of the $1_g(^3P_1)$ and $2_g(^3P_2)$ states have shallow wells of about 100 cm^{-1} at the absorption distances. In Table VIII, we show that 0–0 transition energies calculated for the transitions, $1_g(^3P_1) \leftarrow A(1_u)$ and $2_g(^3P_2) \leftarrow A(1_u)$ and compared with the experimental values.

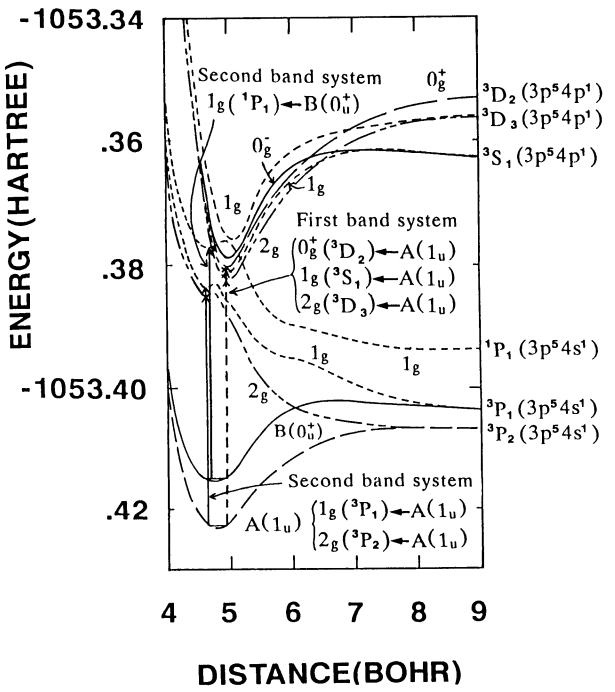

FIG. 4. Vertical transitions corresponding to the absorptions from the $A(1_u)$ and $B(0_u^+)$ states of the Ar excimer.

We note that there is another obscure band in the shorter region of the experimental spectra.[37] The band has three maxima at 11 890 Å (1.043 eV), 11 980 Å (1.035 eV), and 12 110 Å (1.024 eV). We find from our theoretical curves that the transition $1_g(^1P_1) \leftarrow B(0_u^+)$ lies at 1.032 eV (12 014 Å), which is close to the above peaks. So, if these peaks are "real", the $1_g(^1P_1) \leftarrow B(0_u^+)$ transition is a candidate for them. This transition should show rapid relaxation because of the singlet character of the $B(0_u^+)$ state. Thus, we think the measurement of the lifetime for these peaks will clarify the nature of the peaks.

Arai *et al.*[37] observed three peaks at wavelength 9600 Å (1.292 eV), 9754 Å (1.271 eV), and 9883 Å (1.255 eV) as the first absorption band. The former two have shorter lifetimes than that of the last one and are considered as the hot band of the last one.

For the assignment of the 9883 Å peak, we have calculated the potential curves of the Rydberg p excited states by the SAC-CI method and the SO effects are included using the CS method. Some of the lower potential curves of the Rydberg p states are shown in Fig. 4. The lowest three states are candidates for the observed peaks because their transition energies from the $A(1_u)$ state are close to the observed spectra. They are $0_g^+(^3D_2)$, $1_g(^3S_1)$, and $2_g(^3D_3)$ states, which are deeply bound, and originate from the $2^3\Pi_g(^3D)$ state split by the SO interaction. The dipole transitions from the $A(1_u)$ state are allowed as triplet–triplet excitations. The transition energies are compared with the experimental results in Table VIII. We did not identify which state is the upper state of the 9883 Å peak.

We should note here that Kasama, Oka, Arai, Kurusu, and Hama[39] observed highly resolved spectra for the 9883 Å peak of Ref. 37, which involves four fine peaks 9859 Å (10 143 cm^{-1}), 9869 Å (10 133 cm^{-1}), 9881 Å (10 120 cm^{-1}), and 9893 Å (10 108 cm^{-1}). These peaks show curious characters. The energy spacing is about 10 cm^{-1}. The shape and the relative intensity do not change with temperature variation (133 K, 300 K). So it remains unknown what is the origin of these fine structures; rotation, vibration, or different electronic states. Similar fine structures are also observed for Kr_2 and Xe_2.[39]

TABLE VIII. Transition energies of Ar_2 from the $A(1_u)$ state to the upper s and p Rydberg states split by the SO coupling.

Initial state	Final state		Calc (eV)	Exptl[a] (eV)
Second band system				
	Rydberg s			
$A(1_u)$ $v=0$	$1_g(^3P_1)$		1.061	1.001 or 0.9793
$A(1_u)$ $v=0$	$2_g(^3P_2)$		1.022	1.001 or 0.9793
$B(0_u^+)$ $v=0$	$1_g(^1P_1)$		1.032	1.025[b]
				1.035[b]
				1.043[b]
First band system				
	Rydberg p			
$A(1_u)$ $v=0$	$0_g^+(^3D_2)$	$v'=0$	1.185	
$A(1_u)$ $v=0$	$1_g(^3S_1)$	$v'=0$	1.179	1.255
$A(1_u)$ $v=0$	$2_g(^3D_3)$	$v'=0$	1.127	

[a]Reference 37.
[b]These experimental peaks are obscure owing to unsatisfactory signal-to-noise ratio of the detector.

VII. IONIZED STATES OF Ar_2

Rare-gas ions are well known as laser emission species. Reliable potential curves are essential for understanding the dynamics in these species. The adiabatic photoionization spectrum of Ar_2 produced by the supersonic expansion jet was first reported by Ng *et al.*[40] Dehmer and Dehmer[41] observed the vertical photoionization spectra and estimated the spectroscopic properties with the help of the *ab initio* potential curves of Wadt.[42]

We calculate here the potential energy curves of Ar_2^+ by the SAC-CI method and include the SO coupling by the CS method. The potential curves without SO coupling are shown in Fig. 5 and those with SO coupling are shown in Fig. 6. Spectroscopic constants are summarized in Table IX. For the lowest ionized state of Ar_2, the $I(1/2)_u$ state, our vertical ionization potential (IP) is 15.20 eV and is a bit smaller than the experimental value, 15.55 eV. Our adiabatic IP is 14.36 eV and the experimental value is 14.44 eV.[43] Accordingly, our dissociation energy of the $I(1/2)_u$ state (1.11 eV) is smaller than the experimental value, 1.33 eV. The theoretical value due to Wadt (1.19 eV) is also smaller than experiment.

The second lowest state of Ar_2^+, the $I(3/2)_g$ state, has a shallow minimum at $R = 6.0$ bohr with a depth of $D_0 = 0.099$ eV. This value is smaller than the experimental

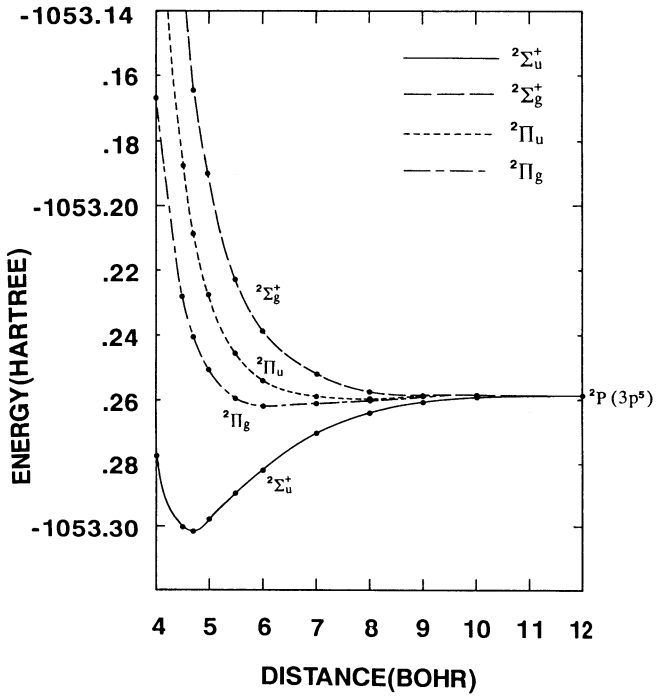

FIG. 5. Potential energy curves of the ionized states of Ar_2 calculated without including SO interactions.

value, 0.14 eV. In Fig. 6, we see a curve crossing at about 6.5 bohr between the $I(1/2)_g$ and $I(3/2)_u$ states. This crossing was also reported by Wadt. At the potential minimum of the ground state, the $I(3/2)_u$ state is lower than the $I(1/2)_g$ state and this is consistent with the ordering of

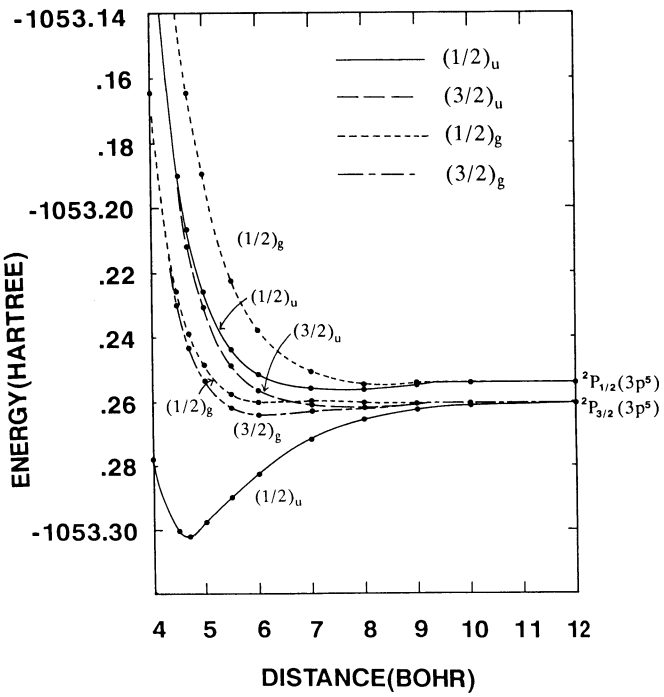

FIG. 6. Potential energy curves of the ionized states of Ar_2 calculated with SO interactions.

TABLE IX. Spectroscopic constants of the ionized states of Ar_2. Experimental results are shown in parentheses.

State	R_{min} (bohr)	Vertical IP(eV)	Adiabatic IP(eV)	ω_e (eV)	$\omega_e\chi_e$ (eV)	D_e (eV)
$I(1/2)_u(^2P_{3/2})$	4.64	15.20 (15.55)[a]	14.36 (14.44)[b]	269.8	2.13	1.11 (1.33)[b]
$I(3/2)_g(^2P_{3/2})$	6.0	15.42 (15.67)[a]	15.39 (15.63)[b]			0.099 (0.14)[b]
$I(3/2)_u(^2P_{3/2})$		15.48				
$I(1/2)_g(^2P_{3/2})$		15.50				
$II(1/2)_u(^2P_{1/2})$	8.0	15.62 (15.87)[a]	15.60 (15.84)[b]			0.064 (0.10)[b]
$II(1/2)_g(^2P_{1/2})$		15.76 (15.99)[a]				

[a]Reference 41.
[b]Reference 43.

the observed vertical IPs. The vertical IPs of the other states are also shown in Table IX and compared with the experimental results. The $II(1/2)_u$ state is found to be a bound state with dissociation energy of 0.064 eV, which is comparable with the experimental value, 0.1 eV.

VIII. CONCLUDING REMARKS

We have calculated the potential energy curves of the ground, excited, and ionized states of Ar_2 by the SAC/SAC-CI method. After including SO coupling, our potential curves for the Rydberg 4*s* excited states show excellent agreement with spectroscopic results. The absorption spectra from the ground state to the $A(1_u)$ state are reproduced to within 340 cm^{-1}. At the dissociation limit, our results agree well with the atomic data to within 420 cm^{-1}. Our dissociation energy is smaller than the experimental value. Among others, new assignments for the absorption spectra from the excited $A(1_u)$ state of the Ar excimer are proposed; they involve the transitions to the different electronic and vibrational states of the 4*s* and 4*p* Rydberg excited states split by the SO coupling. In conclusion, the present results show that the SAC/SAC-CI method gives reliable potential energy curves of both the ground and excited states of the weakly interacting van der Waals systems.

ACKNOWLEDGMENTS

We thank Professor S. Arai of Kyoto Institute of Technology for some useful discussions. We also thank Dr. A. Hiraya and Mr. M. Takahashi at the Institute for Molecular Science for their advice. This study has been supported by a Grant-in-Aid for Scientfic Research from the Ministry of Education, Science, and Culture. The calculations have been carried out at the Computer Center of the Institute for Molecular Science, and at the Data Processing Center of Kyoto University.

[1] Y. Tanaka and K. Yoshino, J. Chem. Phys. **53**, 2012 (1970).
[2] B. P. Stoicheff, *Frontiers of Laser Spectroscopy of Gases*, edited by A. C. P. Alves (Reidel, Dordrecht, 1988).
[3] P. R. Herman, A. A. Madej, and B. P. Stoicheff, Chem. Phys. Lett. **134**, 209 (1987).

[4] P. R. Herman, P. E. LaRocque, and B. P. Stoicheff, J. Chem. Phys. **89**, 4535 (1988).
[5] R. S. Mulliken, J. Chem. Phys. **52**, 5170 (1970).
[6] R. P. Saxon and B. Liu, J. Chem. Phys. **64**, 3291 (1976).
[7] F. Spiegelmann and J. P. Malrieu, Chem. Phys. Lett. **57**, 214 (1978).
[8] M. C. Castex, M. Morlais, F. Spiegelmann, and J. P. Malrieu, J. Chem. Phys. **75**, 5006 (1981).
[9] F. Spiegelmann and F. X. Gadea, J. Phys. (Paris) **45**, 1003 (1984).
[10] J. H. Yates, W. C. Ermler, N. W. Winter, P. A. Christiansen, Y. S. Lee, and K. S. Pitzer, J. Chem. Phys. **79**, 6145 (1983).
[11] F. Grein, S. D. Peyerimhoff, and R. J. Buenker, J. Chem. Phys. **82**, 353 (1985).
[12] F. Grein and S. D. Peyerimhoff, J. Chem. Phys. **87**, 4684 (1987).
[13] H. Nakatsuji and K. Hirao, J. Chem. Phys. **68**, 2053 (1978).
[14] H. Nakatsuji, Chem. Phys. Lett. **59**, 362 (1978); **67**, 329, 334 (1979).
[15] H. Nakatsuji, Chem. Phys. **72**, 425 (1983).
[16] H. Nakatsuji, Theor. Chim. Acta **71**, 201 (1987); H. Nakatsuji, M. Komori, and O. Kitao, *Lecture Note in Chemistry*, 50, edited by D. Mukherjee (Springer, Berlin, 1989), pp. 101–122.
[17] H. Nakatsuji, Program system for SAC and SAC-CI calculations, Program Library No. 146(Y4/SAC), Data Processing Center of Kyoto University, 1985; H. Nakatsuji, Program Library SAC85 (NO. 1396), Computer Center of the Institute for Molecular Science, Okazaki, Japan, 1986.
[18] A. D. McLean and G. S. Chandler, J. Chem. Phys. **72**, 5639 (1980).
[19] S. Huzinaga, J. Andzelm, M. Klobukowski, E. Radzio-Andzelm, Y. Sakai, and H. Tatewaki, *Gaussian Basis Sets for Molecular Calculations* (Elsevier, New York, 1984).
[20] T. H. Dunning, Jr. and P. J. Hay, in *Methods of Electronic Structure Theory*, edited by H. F. Schaefer III (Plenum, New York, 1977).
[21] B. R. Brooks, P. Saxe, W. D. Laidig, and M. Dupuis, Program Library Gamess(No. 481), Computer Center of the Institute for Molecular Science, Okazaki, Japan.
[22] R. S. Mulliken, Phys. Rev. **120**, 1674 (1960).
[23] J. S. Cohen and B. Schneider, J. Chem. Phys. **61**, 3230 (1974).
[24] E. V. Condon and G. H. Shortley, *The Theory of Atomic Spectra* (Cambridge University, London, 1935).
[25] F. Grein, S. D. Peyerimhoff, and R. Klotz, Theor. Chim. Acta **72**, 403, (1987).
[26] C. E. Moore, U.S. Natl. Bur. Stand., Circ. No 467, Vol. I (1949).
[27] H. M. Hulburt and J. O. Hirschfelder, J. Chem. Phys. **9**, 61 (1941); J. Chem. Phys. **35**, 1901 (1961).
[28] D. C. Shannon and J. G. Eden, J. Chem. Phys. **89**, 6644 (1988).
[29] K. P. Killeen and J. G. Eden, J. Chem. Phys. **84**, 6048 (1986).
[30] S. Sauerbrey, H. Eizenhöfer, U. Schaller, and H. Langhoff, J. Phys. B **19**, 2279 (1986).
[31] N. Sato and S. Iwata, J. Comput. Chem. **9**, 222 (1988).
[32] N. Sato, Program Library DIAVIB (No. 1246), Computer Center of the Institute for Molecular Science, Okazaki, Japan, 1985.
[33] Y. Tanaka, W. C. Walker, and K. Yoshino, J. Chem. Phys. **70**, 380 (1979).
[34] A. A. Madej and B. P. Stoicheff, Phys. Rev. A **38**, 3456 (1988).
[35] W. G. Wrobel, H. Rohn, and K. H. Steuer, Appl. Phys. Lett. **36**, 113 (1980).
[36] S. Arai and R. F. Firestone, J. Chem. Phys. **50**, 4575 (1969).
[37] S. Arai, T. Oka, M. Kogoma, and M. Imamura, J. Chem. Phys. **68**, 4595 (1978).
[38] S. Iwata, Chem. Phys. **37**, 251 (1979).
[39] K. Kasama, T. Oka, S. Arai, H. Kurusu, and Y. Hama, J. Phys. Chem. **86**, 2035 (1982).
[40] C. Y. Ng, D. J. Trevor, B. H. Mahan, and Y. T. Lee, J. Chem. Phys. **66**, 446 (1977).
[41] P. M. Dehmer and J. L. Dehmer, J. Chem. Phys. **69**, 125 (1978).
[42] W. R. Wadt, J. Chem. Phys. **68**, 402 (1978).
[43] J. T. Moseley, R. P. Saxon, B. A. Huber, P. C. Cosby, R. Abouaf, and M. Tadjeddine, J. Chem. Phys. **67**, 1659 (1977).